Chapter

Fluorogenic Polyfunctional Coumarin-Based Chemosensors for Multianalyte Detection

Alexander Dubonosov and Vladimir Bren

Abstract

Fluorogenic sensors capable of selective interaction with analyte, which leads to a change in the position or intensity of the fluorescence band, allow to detect ions or molecules *in situ* and *in vivo* and possess high sensitivity and efficiency. Currently, they are widely used in organic, biological, and medical chemistry and environmental sciences for express monitoring of the ionic composition of the medium. They represent a serious alternative to the bulky, expensive, non-transportable technical devices traditionally used for this purpose, such as atomic absorption, atomic emission, and XRF spectrometers. Polyfunctional sensors capable of independent detection of two or more kinds of "guests" from a multiple mixture of cations, anions, or molecules due to specific spectral responses via the same or different channels constitute a rapidly developing area of chemosensory science. This specific feature is associated with the presence of two or more coordination centers in their molecules, or the capability of one center to selectively respond to various analytes with individual spectral changes. Coumarin (2*H*-chromene-2-one) core is one of the most versatile frameworks for the design of fluorogenic polyfunctional chemosensors for multianalyte detection. In this chapter, we report on the review of sensing properties of this group of chemosensors based on functionalized coumarin derivatives, including their applications in bioimaging.

Keywords: coumarin, polyfunctional chemosensor, fluorescence, cations, anions, amino acids, bioimaging

1. Introduction

Chemosensor is a molecule of abiotic origin capable of selective interaction with analyte causing corresponding changes in the physical properties of the initial system (absorption spectra, fluorescence spectra, etc.) [1]. If a change occurs in spectral characteristics, the chemosensor relates to an optical type. There are two main types of optical chemosensors according to their mechanisms of action: chromogenic and fluorogenic [2–4]. In the case of chromogenic chemosensors after binding of analyte, there occurs a change in the electronic absorption spectra of the initial compounds. If this change can be seen with the human eye, we are dealing with a "naked-eye" chemosensor. Fluorogenic chemosensors can change their fluorescence spectrum after the interaction of analyte with receptor. It is highly desirable that this process is also accompanied by a "naked-eye" effect—contrast change in the

color of emission. Chromogenic and fluorogenic chemosensor systems are widely used in organic, biological, and medical chemistry and environmental sciences for monitoring cations and anions. They represent a real alternative to the bulky, expensive, non-transportable technical devices, such as atomic absorption, atomic emission, and XRF spectrometers, that are traditionally used for this purpose. Of special efficiency are fluorogenic sensors, which use fluorescence for detection of various analytes, allow measurements *in situ* and *in vivo,* and are distinguished by highest sensitivity and selectivity. Recently a new scientific area in chemosensorics arose, which is associated with the design of poly- and bifunctional sensors capable of independent detection of two or more kinds of ions-"guests" due to the specific spectral responses via the same or different channels [5–8]. Using a single molecule possessing different reactions against multiple analytes is cost-effective and useful for practical applications.

Herein we report on the review of spectral, fluorescent, and sensing properties of new representatives of this group of chemosensors based on functionalized coumarin derivatives, including their applications in bioimaging.

Coumarins (derivatives of 2*H*-chromene-2-one) constitute a comprehensive group of extensively studied heterocyclic compounds in organic, physical, and medical chemistry [9, 10]. Some coumarins have been selected as privileged scaffolds for drug design [11–13], and a number of antitumor, antiproliferative, antioxidant, antifungal, anti-inflammatory, and antiviral agents have been obtained on their basis [14–19]. As a rule, substituted coumarins possess fluorescence in the visible part of the spectrum, as well as other useful photophysical properties. They are widely used in laser dyes, light-emitting devices, and solar cells. In addition, 2*H*-chromene-2-one is considered one of the most versatile frameworks for design of fluorescent, chemo- and biosensor systems [20–23].

There are several excellent reviews devoted entirely or partially to coumarin chemosensors [24–28], but polyfunctional coumarin-based sensors for multianalyte detection until now have not been considered.

2. Sensing of multiple metal cations

Fluorescent polyfunctional sensors for detection of metal cations must contain a metal chelating or binding fragment attached to a coumarin core capable of absorbing and emitting light. The formation of complexes with ions should cause a change in the electronic structure or molecular conformation, which should result in an increase or decrease in the emission intensity.

A fluorescent sensor **1** (**Figure 1**) demonstrates a high selectivity toward Al^{3+} and Zn^{2+} in the presence of many various metal cations. Aluminum is the third most

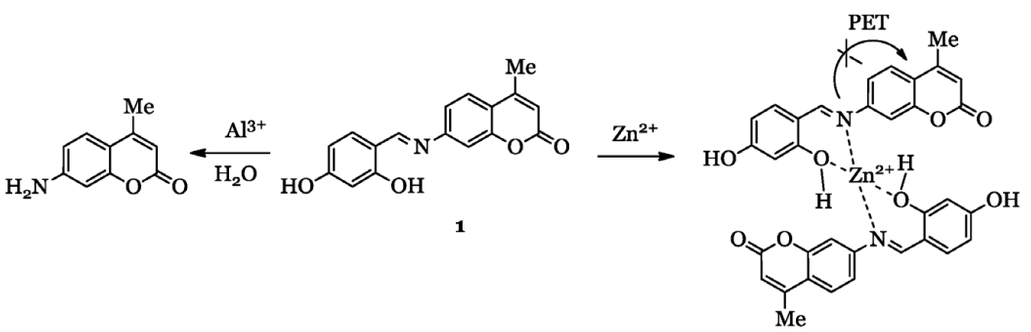

Figure 1.
Detection of Al^{3+} and Zn^{2+} by sensor **1**.

common element in the earth's crust. It is used in food additives and cookware, although its cations are highly toxic and may be associated with Parkinson's and Alzheimer's diseases, microcytic anemia, dialysis dementia, and osteomalacia. Zinc is the second most abundant *d*-metal cation, which plays a crucial role in gene transcription, regulation of metalloenzymes, and transmission of nerve signals. However, it has some toxicity and its excess in living cells can cause neurodegenerative disorders, epilepsy, and seizures.

A new emission band at 427 nm (an increase in intensity ~500 times) in the presence of Al^{3+} in ethanol-water mixture appears due to hydrolysis of imine **1**. The detection limit (LOD) was calculated to be 3.7×10^{-6} M. Detection of Zn^{2+} leads to a substantial initial fluorescence intensity enhancement at 489 nm due to the inhibition of PET process (photoinduced electron transfer) [29].

Coumarin **2** exhibits a significant enhancement of fluorescence intensity upon detection of Zn^{2+} (535 nm, 270-fold) or Al^{3+} ions (518 nm, 230-fold) in MeOH/H_2O mixture with LODs 3.75×10^{-8} and 1.14×10^{-8} M, respectively [30]. It has been shown that the sensing mechanism is based on inhibition of ICT process (intramolecular charge transfer) (**Figure 2**).

Compound **2** possesses a low toxicity and was used for fluorescent bioimaging of Zn^{2+} and Al^{3+} cations in PC12 cells.

Coumarin-crown compound **3** exhibits a high selectivity for the detection of Al^{3+}, Cu^{2+}, and Mg^{2+} in ethanol [31] (**Figure 3**). Copper(II) cations play an important role in biological systems. Their lack can lead to anemia and low white cell amount while an excess is accountable for neurodegenerative, Alzheimer's, and Wilson's diseases. Magnesium(II) cations are among the most abundant divalent cations in living cells. They are responsible for the formation of bone tissue, enzymatic biochemical reactions, cell proliferation, and DNA conformation stabilization, whereas their excessive concentration in the cytosol can lead to diabetes, hypertension, epilepsy, and Alzheimer's disease.

While copper(II) is identified by color change of solution from a slight yellow to orange, Al^{3+} and Mg^{2+} ions cause a significant fluorescence enhancement at 592 nm and 547 nm with low detection limits of 0.31 μM and 0.23 μM, respectively.

Chemosensor **4** was developed for dual detection of Fe^{3+} and Zn^{2+} ions [32] (**Figure 4**). Iron(III) is the most common *d*-metal cation in the human organism, it plays a significant role in many enzymatic reactions and in specialized transport and storage of proteins. Its lack can cause anemia, diabetes, hemochromatosis, and Parkinson's disease. Further development of this work led to the obtaining of a polyfunctional sensor **5** for Fe^{3+}, Zn^{2+}, and Cu^{2+} cations [33] (**Figure 4**). Formation of complex with Fe(III) ion and **4** or **5** is accompanied by a contrast color change from colorless to deep yellow.

Upon interaction with Zn^{2+} in CH_3OH/H_2O mixture, the emission intensity at 484 nm increases by five times compared to other metal ions. The LOD was found to be ~10^{-6} M. Since Cu^{2+} is a paramagnetic ion, its presence in the solution causes

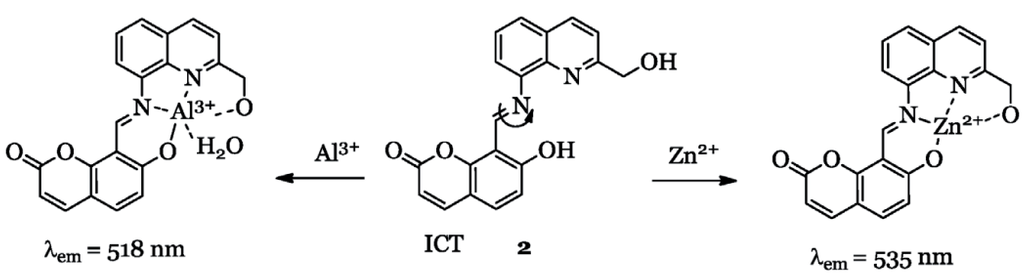

Figure 2.
Proposed scheme of detection Zn^{2+} and Al^{3+} by sensor **2**.

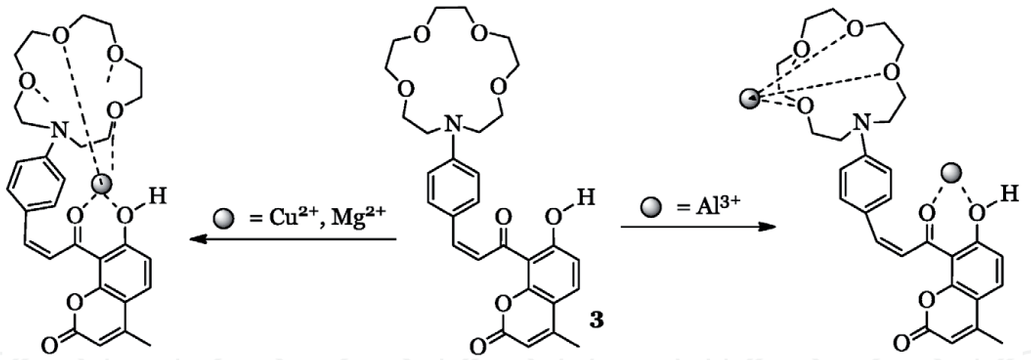

Figure 3.
Possible binding mechanisms of Cu^{2+}, Mg^{2+}, and Al^{3+} by coumarin **3**.

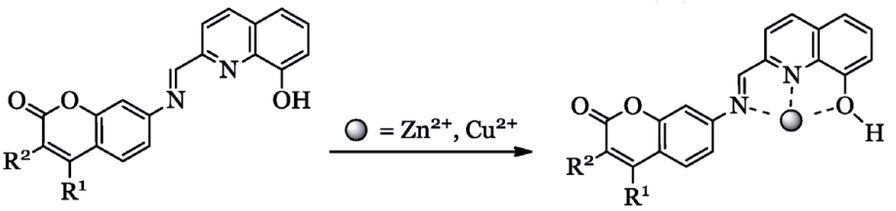

4 ($R^1 + R^2 = C_4H_4$); **5** ($R^1 = CF_3$, $R^2 = H$)

Figure 4.
Complexation of coumarins **4** *and* **5** *with Zn^{2+} and Cu^{2+}.*

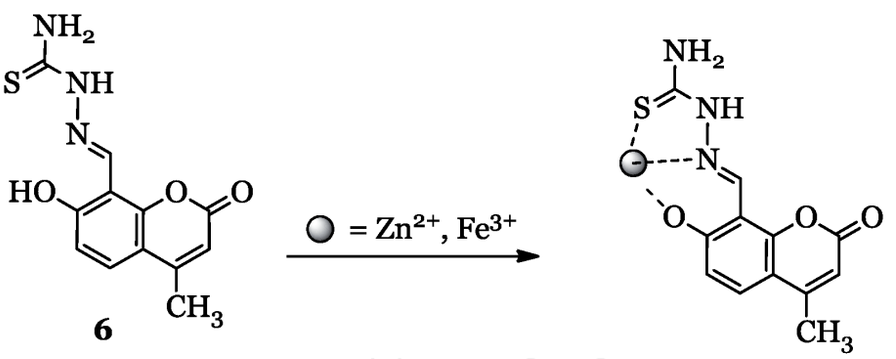

Figure 5.
Sensing of Fe^{3+} and Zn^{2+} by coumarin **6**.

a substantial quenching of initial fluorescence of **4** and **5**. The detection limit was calculated and found to be ~10^{-5} M.

A similar approach was used in design of a dual chemosensor **6** [34] (**Figure 5**). While Fe^{3+} ions in EtOH/H_2O solution cause only a visible color change from colorless to brown, the addition of Zn^{2+} ion resulted in 45-fold enhancement in the fluorescence intensity at 473 nm. The LOD was found to be 0.6 × 10^{-8} M.

Application of compound **6** as bioimaging fluorescent sensor for detection of Zn^{2+} in human cancer cells was also observed by fluorescent cell imager (**Figure 6**).

Chemosensor **7,** as well as **4** and **5**, in water (1% EtOH) solution demonstrates the quenching of the fluorescent properties when adding Cu(II) ions and significantly increases the emission intensity in the presence of Zn(II) ions [35] (**Figure 7**).

When Cu^{2+} and Zn^{2+} were monitored by sensor **7**, the LODs were 141 nM and 72 nM, respectively. About 85% of cells survive upon addition of 80 μM of **7** indicating its hypotoxicity and possibility of using it for cell imaging (**Figure 8**).

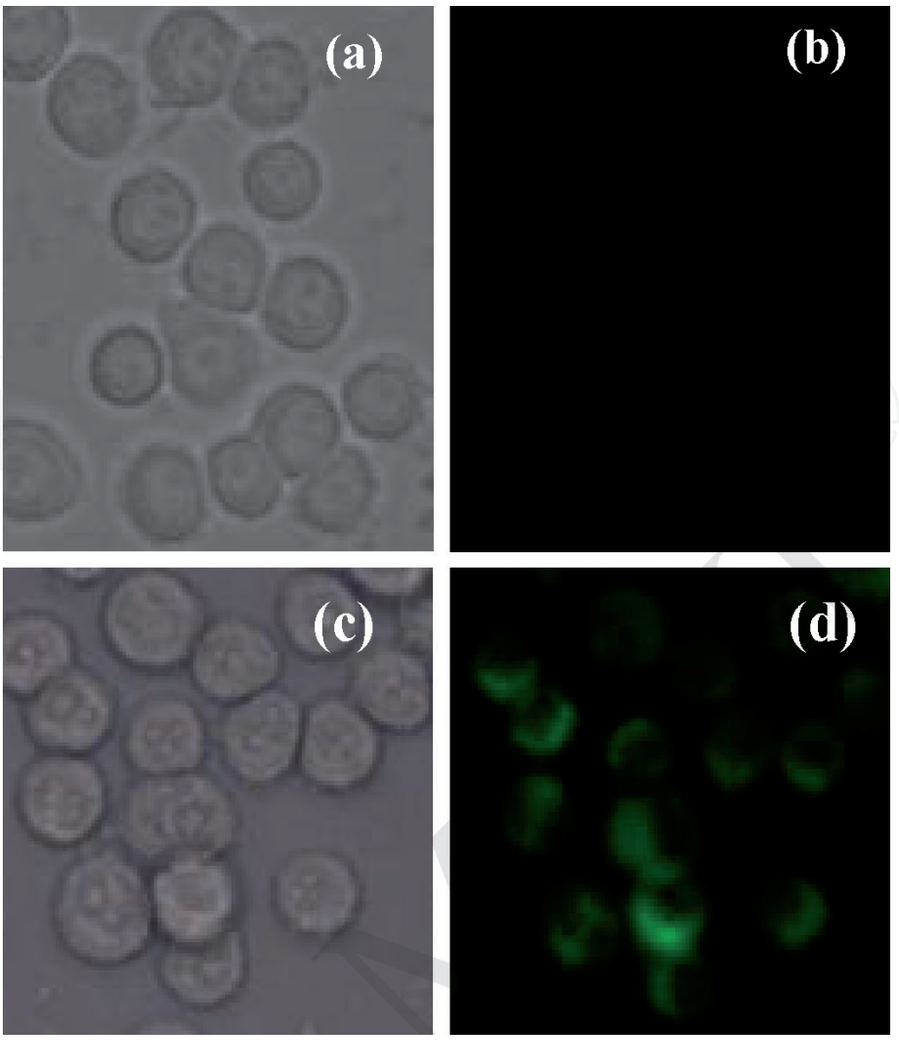

Figure 6.
Fluorescence microscopic images of cancer cells treated with coumarin **6** *(5 μM) in bright field (a) and merged field (b), pretreated with* **6** *(5 μM) followed by addition of 10 μM of Zn^{2+} in bright field (c) and merged field (d) [34].*

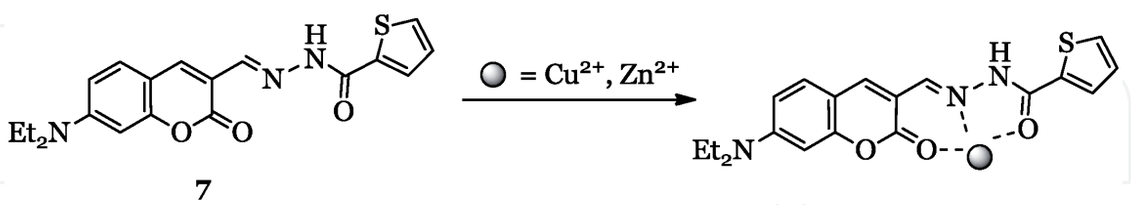

7

Figure 7.
Binding modes of Cu^{2+} and Zn^{2+} by coumarin **7**.

Coumarin-naphthalene chemosensor **8** in the CH_3OH/H_2O mixture acts as a chemodosimeter for Ag^+ ions and a fluorescent sensor in relation to Cu^{2+} ions [36]. Silver is a potentially toxic and potentially carcinogenic element. It is known that Ag^+ can react with proteins in the body, block thiol groups of enzyme systems, and inhibit tissue respiration. Excessive concentration of Ag^+ ions in the body can lead to brain damage. Compound **8** possesses fluorescence at 480 nm, and its intensity is enhanced upon the addition of Cu^{2+} ions. However, the fluorescence intensity is quenched upon addition of Ag^+ ions due to irreversible desulfurization (**Figure 9**).

The detection limits of **8** are 8.1×10^{-9} M and 44.0×10^{-9} M for Cu^{2+} and Ag^+ ions, respectively. Compound **8** represents a safe and nontoxic to live cells

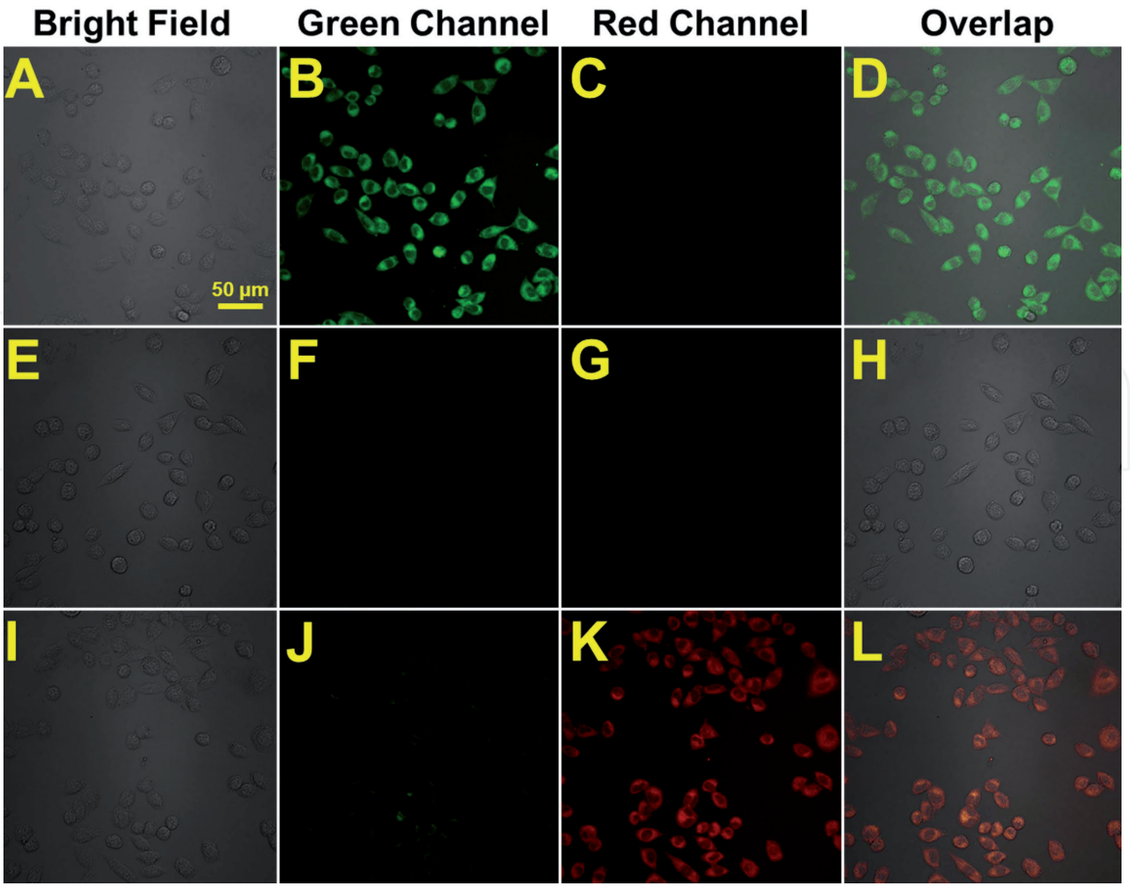

Figure 8.
Relative confocal fluorescence images of MRC-5 cells under different conditions with **7**. *MRC-5 cells treated with 5 μM of* **7** *(A–D), then further incubated with 5 μM of Cu(II) (E–H) and Zn(II) (I–L) ions for 10 min. Fluorescence images from left to right: Bright field, green channel, red channel, and overlap [35].*

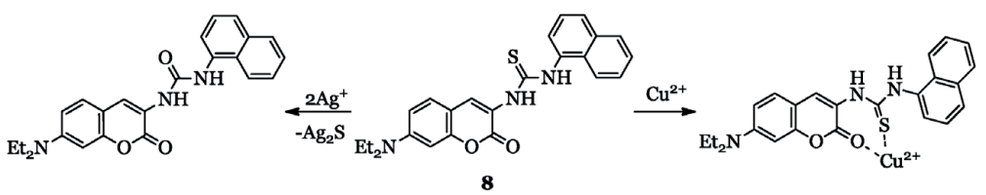

Figure 9.
Chemodosimeter and chemosensor properties of **8**.

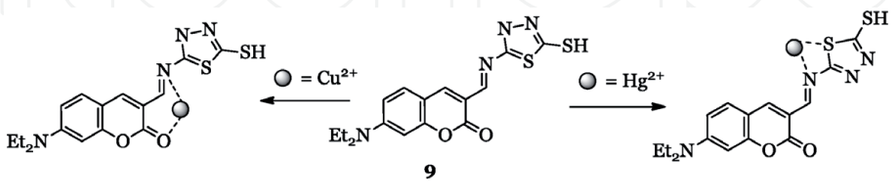

Figure 10.
The binding modes of **9** *with* Cu^{2+} *and* Hg^{2+} *ions.*

biosensor. Only weak emission was observed in human osteosarcoma cells U-2 OS when exposed to **8**, while strong blue and green fluorescence was observed upon addition of Cu^{2+} ions.

A dual-function coumarin chemosensor **9** could monitor Cu^{2+} and Hg^{2+} in CH_3CN/H_2O mixture [37]. The addition of Cu(II) cations changes the solution color from yellowish-brown to yellowish-green, while Hg^{2+} causes the fluorescence intensity enhancement at 572 nm (**Figure 10**).

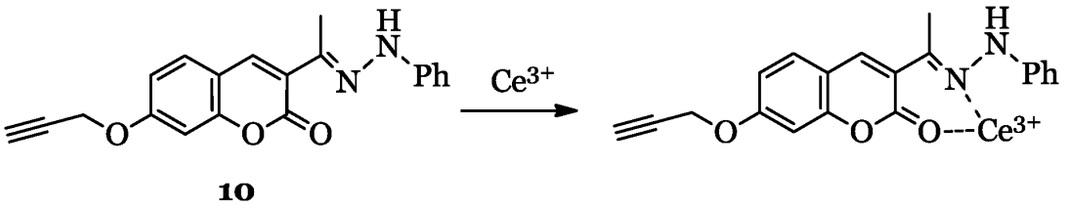

10

Figure 11.
Complexation of **10** *with* Ce^{3+}.

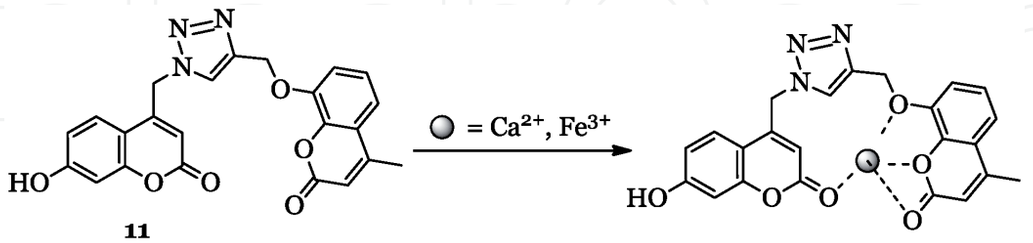

11

Figure 12.
Sensing of Ca^{2+} *and* Fe^{3+} *by* **11**.

The detection limit for Hg^{2+} was calculated to be 2.96×10^{-7} M.

Coumarin chemosensor **10** for detection of Ag^{+} and Ce^{3+} ions in an aqueous solution was developed [38]. Cerium is the most abundant of the lanthanides and refers to the conventionally toxic rare earth ultramicroelements. In the presence of Ag^{+}, the color of the solution of **10** in EtOH/H2O changes from pale yellow to brown. The addition of Ce^{3+} ion results in the substantial emission intensity enhancement at 350 nm (**Figure 11**).

The detection limit of Ce^{3+} ion by the sensor **10** was estimated to be 2.07×10^{-7} M.

Selective fluorescent coumarin-triazole chemosensor **11** toward Ca^{2+} and Fe^{3+} ions was synthesized [39]. Calcium(II) plays an important role in bone formation and as a second messenger in neurotransmitter release from neurons, in contraction of all muscle cell types and in fertilization. Inhibition of the PET process in **11** with Ca^{2+} ions leads to the fluorescence intensity increase at 473 nm, whereas complexation with Fe^{3+} causes its almost complete quenching (**Figure 12**).

The limit of detection was found to be 0.14 μM for Ca^{2+} and 0.25 μM for Fe^{3+}.

3. Sensing of multiple anions

A very small number of fluorogenic polyfunctional coumarin-based chemosensors for multianalyte detection has been created so far. This is due to the fact that the recognition of anions is in principle a very difficult problem, since charges of anions are more diffused than those of cations, which leads to rather weak electrostatic interactions between anions and receptor part of the sensor. As a result, the receptors connected with the coumarin core must have the ability to either form of hydrogen bonds with anions up to complete deprotonation, or to nucleophilic addition reactions. Anions play an important role in medicine, biology, and industry. A deficiency of fluoride ions can cause gum disease and osteoporosis, and an excess leads to fluorosis due to its nephrotoxic action. Both excess and deficiency of bromide and iodide anions affect the functioning of the thyroid gland and can cause serious diseases. Acetate anion is involved in various metabolic processes. Cyanide ion is highly toxic to humans even in small concentrations due to its strong interaction with cytochrome-oxidase.

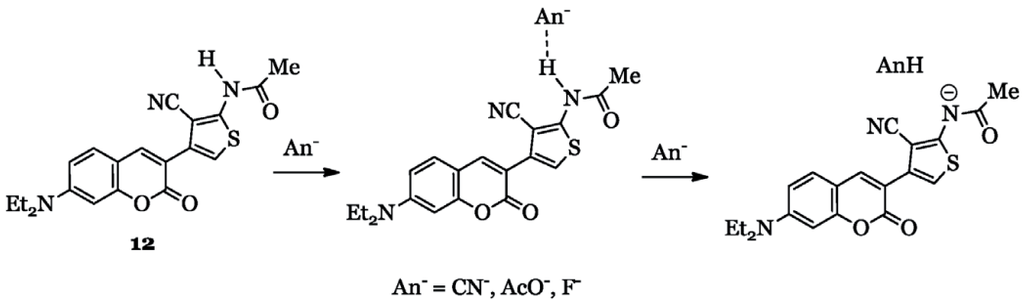

Figure 13.
Binding mode of coumarin **12** *with* CN^-, F^-, *and* AcO^- *in DMSO.*

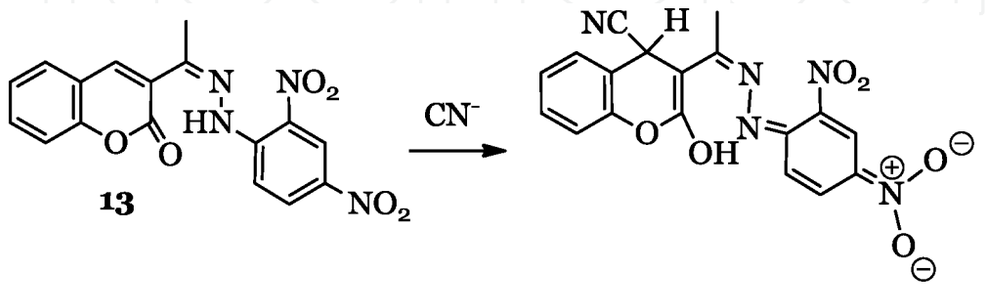

Figure 14.
The possible mode of binding for **13** *and* CN^-.

Coumarin chemosensor **12** is capable of detecting CN^-, F^-, and AcO^- in the presence of other ions-competitors [40]. Only cyanide anions caused a significant increase in the fluorescence intensity at 506 nm. However, only emission quenching was observed upon addition of CN^-, F^-, and AcO^- to the solution of **12** in DMSO. According to ^1H NMR titration data, this is due to the removal of the NH proton and the formation of the anionic form of **12** (**Figure 13**).

The fluorogenic and chromogenic chemosensor **13** in acetonitrile showed a change in the solution color upon addition of F^- and AcO^- ions from a yellow-green to red and orange, respectively [41]. In an aqueous medium, **13** selectively reacted with cyanide anion via a nucleophilic addition reaction, and the nonfluorescent solution turned a fluorescent blue-green at 495 nm (**Figure 14**).

The addition of cyanide anions to an aqueous solution of **13** containing blood plasma caused a significant fuorescence enhancement at 450 nm by ~7.7 times and a change in the nonfluorescent color of solution to blue. The LOD to detect cyanide anion in blood plasma was found to be 0.37 mM.

Coumarin-thiazole chemosensor **14** for CN^-, F^-, and AcO^- ions was synthesized [42]. Compound **14** demonstrated a color change in DMSO upon addition of these anions from yellow to deep red in the visible region and yellow fluorescence with CN^-.

^1H NMR and DFT calculation data correspond to the deprotonation mechanism, while for CN^- it is simultaneously supplemented by the addition reaction (**Figure 15**).

Coumarin **15** with the structure analogues to **14** was designed and synthesized for the selective detection of fluoride and cyanide anions [43]. Chemosensor **15** in acetonitrile selectively reacts with F^- via deprotonation mode, accompanied by a change in the color of the solution from colorless to deep red and a significant enhancement in the intensity of a yellow fluorescence. However, in an aqueous medium a substantial increase in the emission intensity at 506 nm was registered only in the presence of CN^- ions (**Figure 16**).

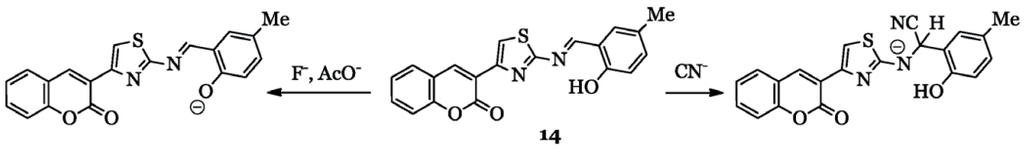

Figure 15.
Detection mechanisms of **14** *with* CN^-, AcO^-, *and* F^-.

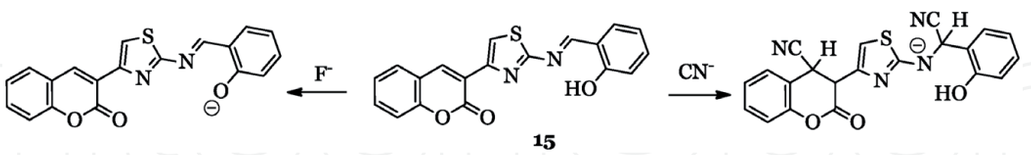

Figure 16.
Binding modes of **15** *with* F^- *and* CN^-.

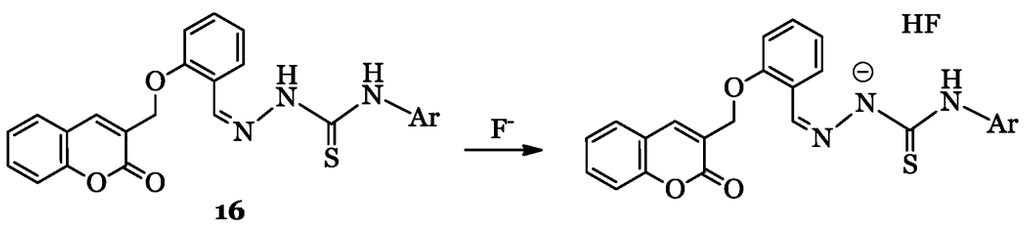

Figure 17.
Sensing of F^- *by* **16**.

The LOD of fluoride ions in organic medium is 0.72 μM, while for cyanide ions in aqueous environment the LOD is 2.7 μM.

Coumarin thiosemicarbazones **16** act via naked-eye and fluorescence mechanisms [44] (**Figure 17**). They were found to be selective chemosensors for F^- with 1:1 receptor-anion ratio due to the appearance of a new emission band at 452 nm upon the addition of TBAF.

4. Sensing of metal cations and anions

As a rule, polyfunctional coumarin sensors for detection of metal cations and anions should include sites of various nature for the detection of these types of ions. Another displacement approach is based on the initial *in situ* formation of a complex with a cation, which then interacts with the anion, releasing the original sensor.

Diethylamine coumarin derivatives **17** and **18** were designed and synthesized to detect cyanide and copper(II) ions [45, 46]. The sensing mechanism is associated with the formation of a covalent bond between cyanide anions and 4-C carbon atom of coumarin (**Figure 18**). Red fluorescence of **17** at 669 nm is completely quenched, which is clearly visible to the naked eye. Complexation of **17** with Cu^{2+} exhibits color change from red to maroon and decreases the fluorescence intensity. LODs are 0.018 μM and 0.004 μM for CN^- and Cu^{2+}, respectively. Compound **18** also recognizes cyanide anions based on nucleophilic addition and copper(II) cations based on coordination reaction (**Figure 18**). However, in this case CN^- causes an obvious enhancement of fluorescence at 473 nm.

The detection limits of the compound **18** are 0.0071 μM (CN^-) and 0.014 μM (Cu^{2+}).

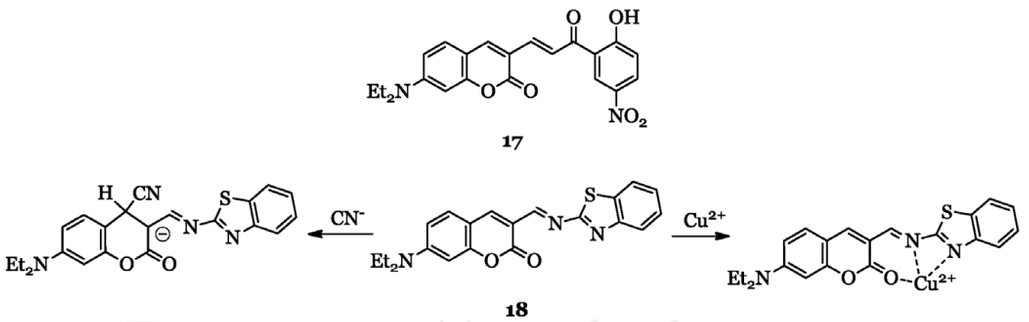

Figure 18.
Structures of **17** *and* **18** *and the proposed sensing mechanism of* **18**.

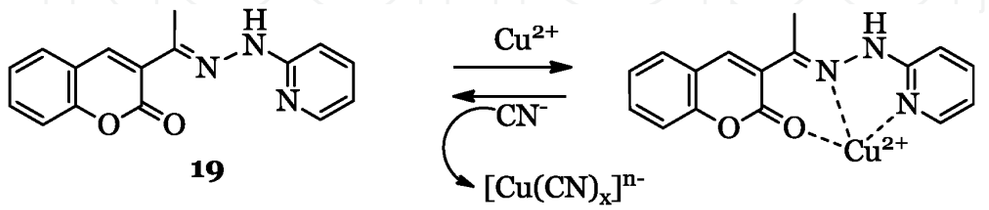

Figure 19.
Sensing of Cu^{2+} *and* CN^- *by* **19**.

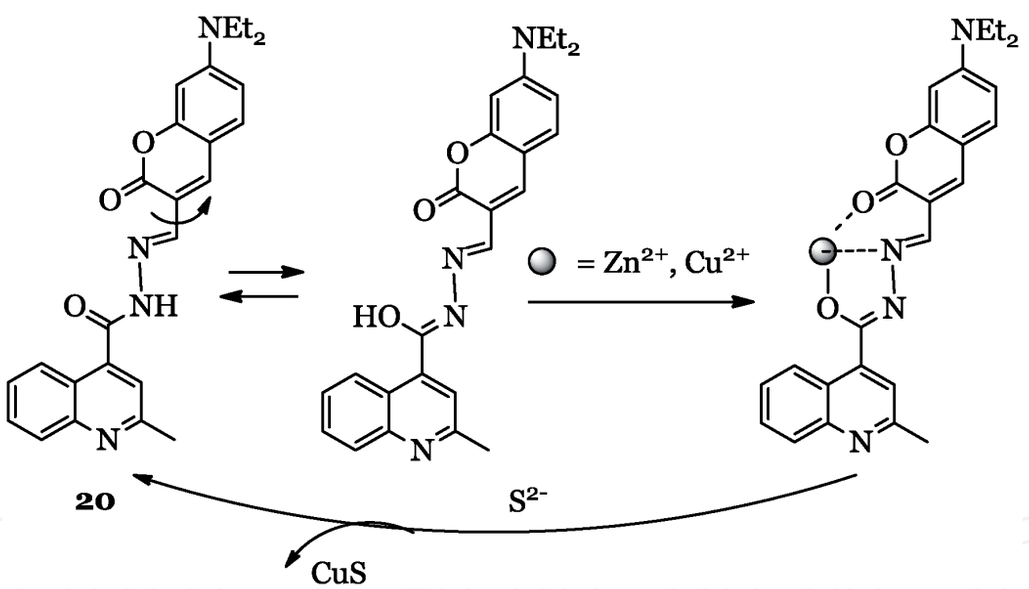

Figure 20.
Sensing of Zn^{2+}, Cu^{2+}, *and* S^{2-} *by* **20**.

Coumarin-based chemosensor **19** was obtained for selective fluorescent recognition of Cu^{2+} in MeOH/H_2O mixture and subsequent detection of CN^- via displacement approach [47]. Compound **19** demonstrates strong emission at 448 nm, which is selectively quenched upon addition of Cu^{2+} due to the formation of the complex (**Figure 19**) with the LOD of 3.76×10^{-7} M.

This *in situ* prepared chelate easily reacts with CN^- to form a very stable complex $[Cu(CN)_x]^{n-}$ and the initial fluorescence is restored with the LOD of 1.35×10^{-6} M, which is much lower than the WHO limit of CN^- (1.9 μM) for drinking water.

Coumarin **20** exhibits a significant increase in fluorescence intensity at 514 nm in the presence of Zn^{2+} ions, which is associated with the cessation of C=N isomerization process [48]. The detection limit reached at 5.76×10^{-7} M. As expected, the

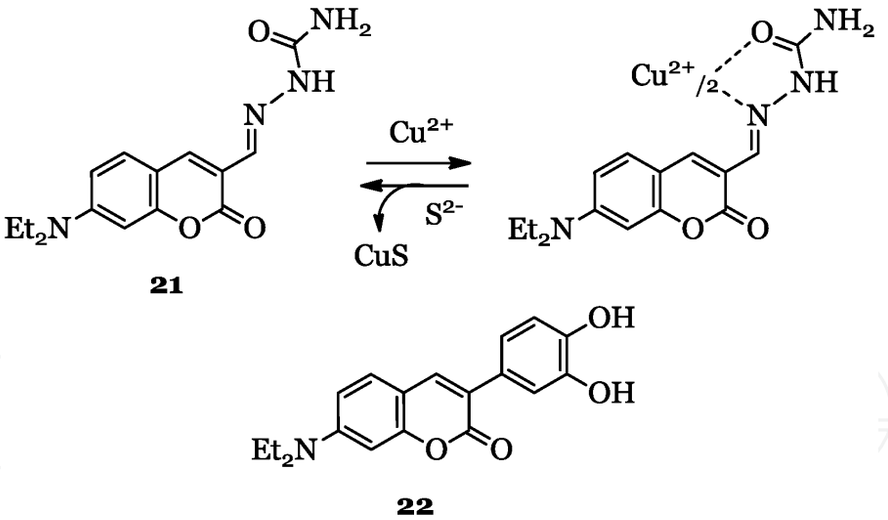

Figure 21.
Structures of **21** *and* **22** *and the proposed sensing mechanism of* **21**.

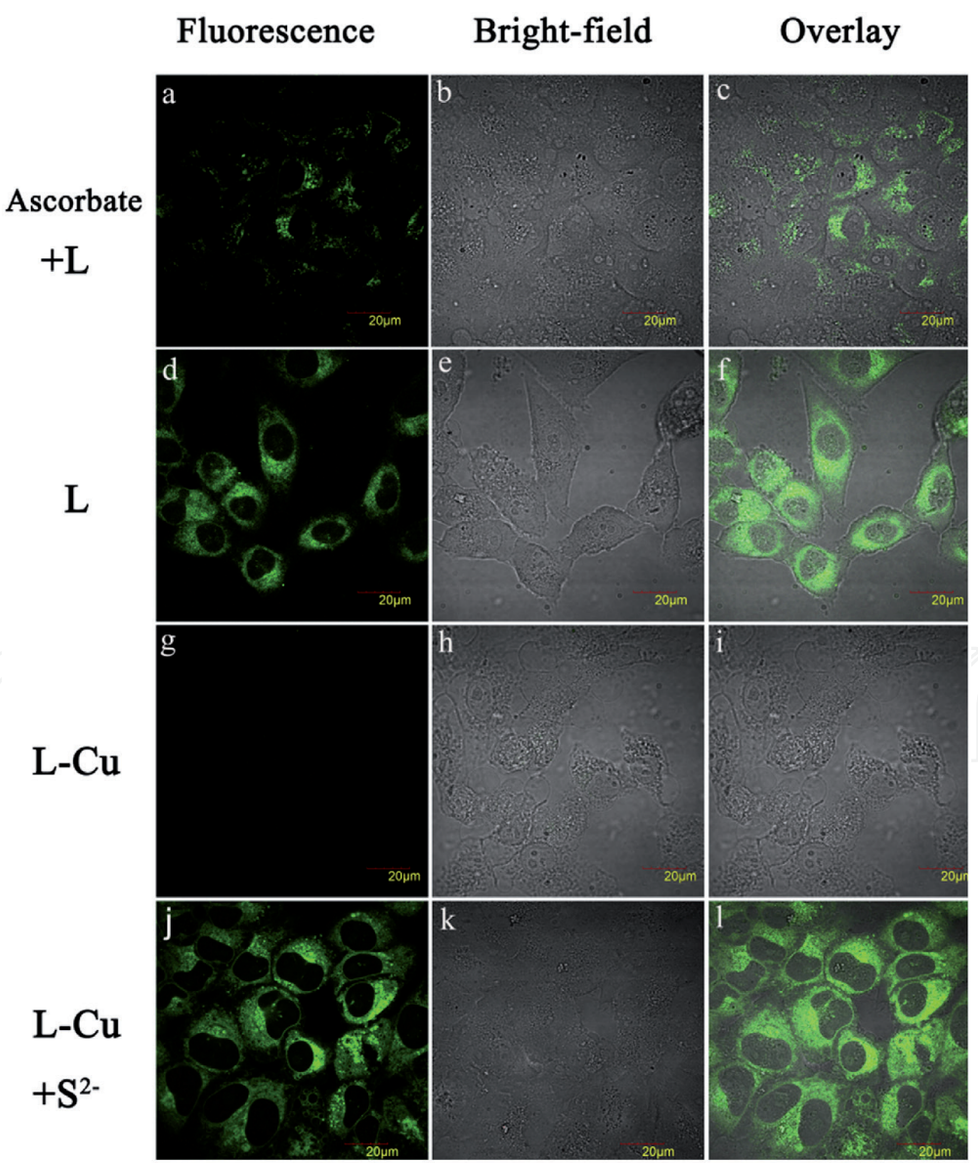

Figure 22.
Confocal fluorescence imaging of A375 cells. Cells incubated with ascorbate (1 mM) for 3 h and stained with **21** *(***L***, 10 μM) for 30 min (a–c); cells treated with* **21** *(10 μM) for 30 min (d–f); cells treated with* **21** *(10 μM) and* cu^{2+} *(20 μM) for 30 min (g–i); cells treated with* **21***-Cu (10 μM) and* S^{2-} *(20 μM) for 30 min (j–l) [49].*

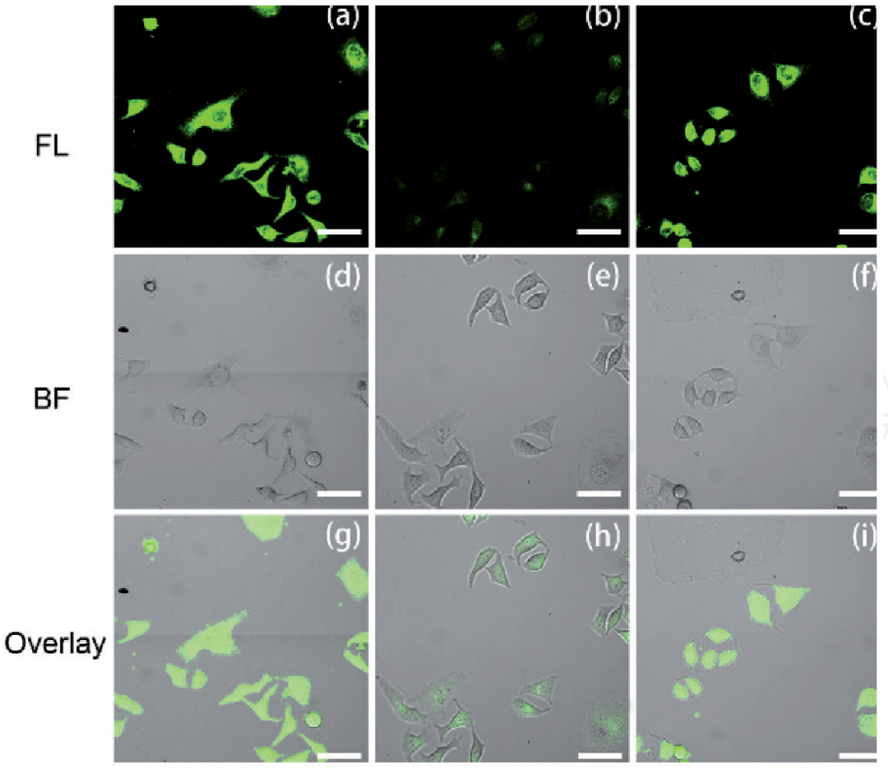

Figure 23.
Confocal fluorescence images of HeLa cells. (a) Cells incubated with **22** *(10 mM) for 30 min. (b) Cells incubated with* **22** *(10 mM) for 30 min, further incubated with Cu^{2+} (20 mM) for 30 min. (c) Cells incubated with* **22** *(10 mM) for 30 min, further incubated with Cu^{2+} (20 mM) for 30 min, and then incubated with S^{2-} (40 mM). (d-f) Bright-field pictures. (g-i) Overlapped pictures. Scale bar, 40 mm [50].*

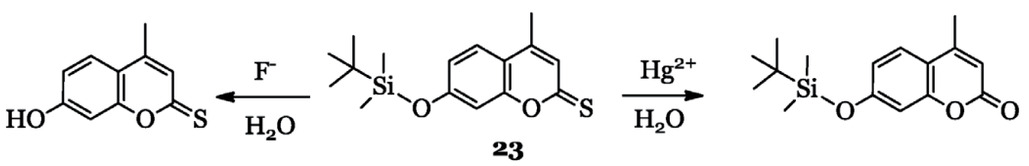

Figure 24.
Irreversible chemodosimeter sensing of Hg^{2+} and F^- by **23**.

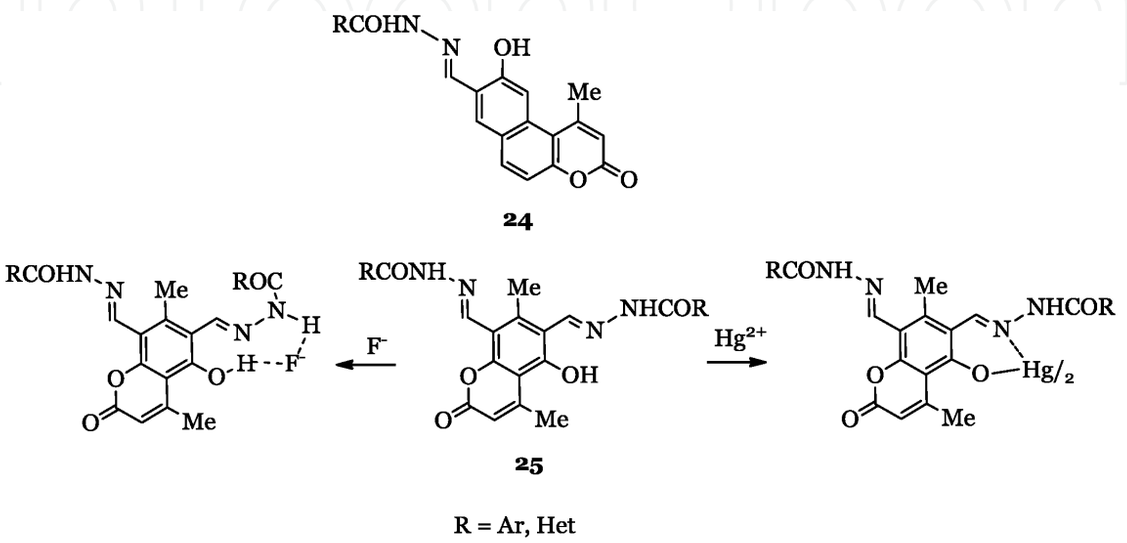

Figure 25.
Structures of **24** *and* **25** *and a tentative scheme of sensing Hg^{2+} and F^- ions by the bifunctional chemosensors* **25**.

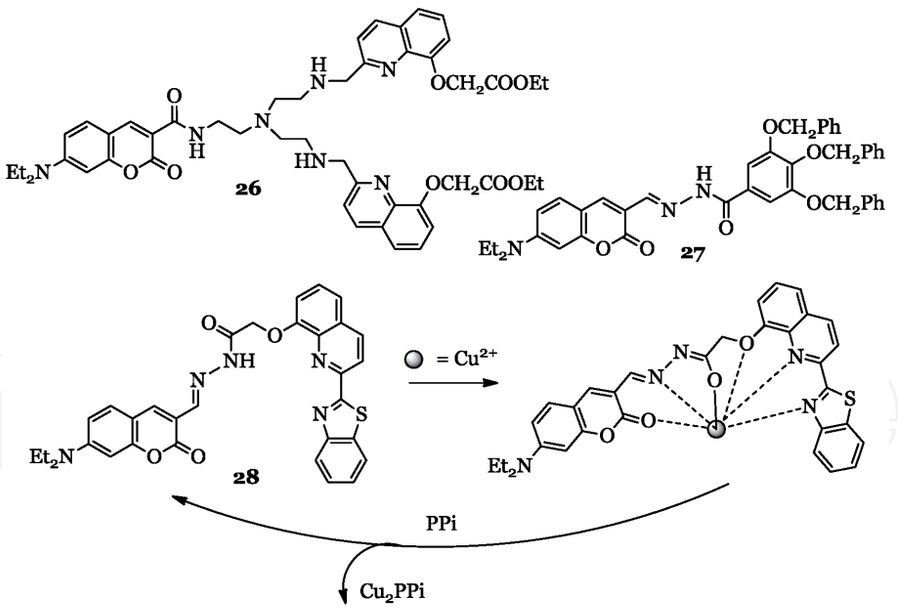

Figure 26.
Structures and sensing mechanism of **26–28.**

Cu(II) cations almost completely quenched this fluorescence due to their inherent paramagnetic properties (**Figure 20**). The LOD reached at 3.1×10^{-7} M.

Thus, prepared *in situ* complex with copper regenerates the initial fluorescence of **20** upon addition of S^{2-} even in the presence of F^-, Cl^-, Br^-, and I^- due to the formation of a very stable CuS. The LOD for S^{2-} was measured to be 1.9×10^{-5} M.

Further development of this approach has been applied in the design of chemosensory systems **21** and **22** suitable for intracellular biology applications. Coumarin **21** demonstrates an intensive emission at 516 nm [49, 50]. The fluorescence intensity decreases (~14-fold) upon addition of Cu^{2+} and reappears in the presence of S^{2-} anions (**Figure 21**). The LOD toward Cu(II) was found to be 2×10^{-8} M, which is lower than the most of the values reported in literature, and toward S^{2-}—6×10^{-8} M.

For the purpose of Cu^{2+} and S^{2-} biovisualization, confocal fluorescent imaging was performed using A375 cells. It is clearly visible in the dark field images that green fluorescence is significantly quenched by Cu^{2+} and restored after subsequent treatment by S^{2-} (**Figure 22**). The A375 cells were viable and maintained good shape in the entire process of this experiment, which means that **21** can successfully cross the cell membrane.

Similar results were obtained for **22**. HeLa cells were incubated with **22** (10 mM) at 37°C for 30 min and displayed bright green fluorescence (**Figure 23**). After incubation with Cu^{2+} for another 30 min, the emission of cells decreased. Upon addition of S^{2-} anions, the fluorescence intensity was restored. This indicates that **22** represents a potent candidate for sensing intracellular Cu^{2+} cations and S^{2-} anions in living cells.

The chemodosimeter approach was exploited for detection of Hg^{2+} and F^- ions by a simple coumarin derivative **23** [51] (**Figure 24**).

Upon addition of Hg^{2+} and F^- ions, **23** underwent desulfurization and desilylation to induce an increase in the fluorescence intensity at 491 nm and 526 nm, respectively.

Aroylhydrazones **24** and bis-aroylhydrazones of coumarin **25** display the properties of bifunctional fluorescent and colorimetric naked-eye chemosensors for mercury(II) cations and fluoride anions detection [52–54] (**Figure 25**).

The addition of Hg^{2+} ions in acetonitrile solution of **25** allows to observe a distinct naked-eye effect with the change of color from pale-yellow to bright-orange.

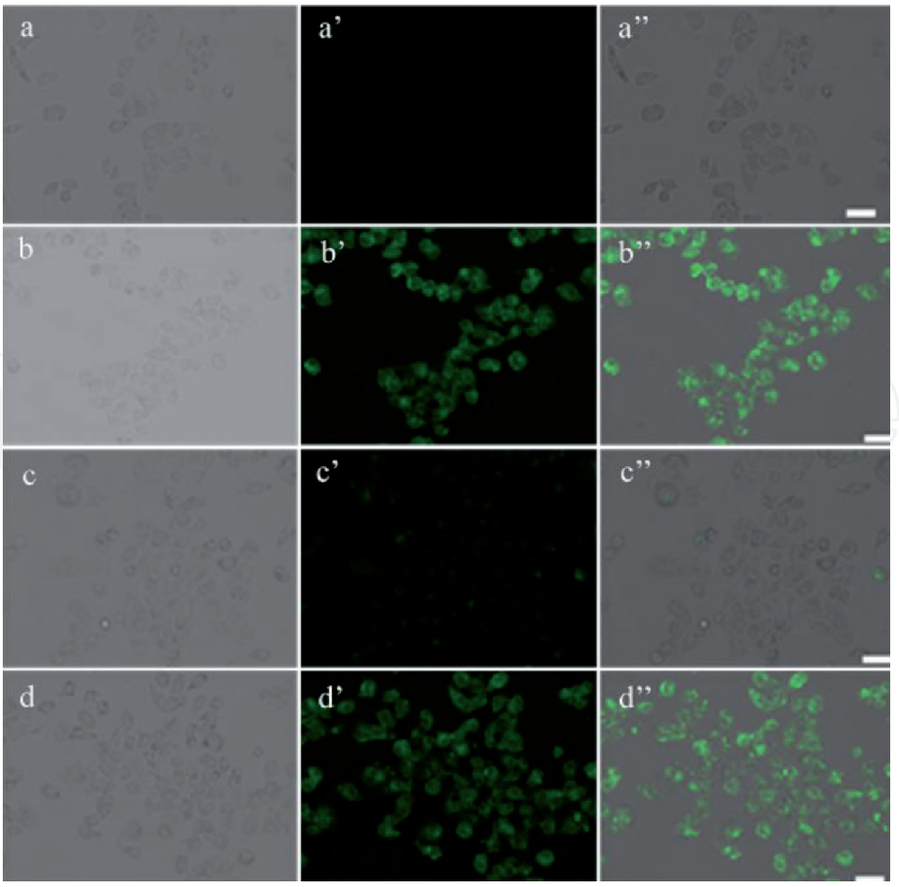

Figure 27.
Bright-field (a, b, c, d), fluorescence (a′, b′, c′, d′), and confocal fluorescence microscope (a″, b″, c″, d″) images of HeLa cells: Blank cell (a, a′, a″); cells treated with 5 μM **28** *(b, b′, b″), then treated with 50 μM Cu^{2+} (c, c′, c″) and further treated with 50 μM PPi (d, d′, d″). the scale bar was 50 μm [57].*

Simultaneously, the initial fluorescence is almost completely quenched. The LOD of mercury(II) cation sensing is 2.7 μM. In the presence of fluoride, cyanide, and acetate anions, a new absorption maximum in the visible spectral region appears. Furthermore, the formation of complex of **25** with fluoride anions is accompanied by the decrease in the relative intensity of the initial fluorescence I_0/I in ≈22 times.

Coumarin-based chemosensors **26–28** with complex chemical architecture were designed and synthesized for selective sequential recognition of Cu^{2+} and pyrophosphate anion (PPi) [55–57]. PPi is the main product of adenosine triphosphate hydrolysis in living cells, which is involved in important metabolic processes. The structures of **26–28** and the sensing mechanism are shown in **Figure 26.** These compounds demonstrate on–off fluorescence quenching toward the Cu^{2+} cation due to the formation of complexes that show off–on fluorescence enhancement upon addition of PPi over many competitive anions.

Chemosensor **28** showed sequential on–off–on fluorescent bioimaging of Cu^{2+} and PPi in HeLa cells. After the addition of **28**, the intense green fluorescence appeared (**Figure 27**). Cells incubated with Cu(II) cations efficiently quenched this emission, which was restored when treated with PPi. These data indicate that the sensor **28** possesses good cell permeability and can be used for bioimaging in live cells. The LOD for Cu^{2+} is 0.06 μM and for PPi it is 0.01 μM.

5. Sensing of metal cations and amino acids

Polyfunctional coumarin sensing of amino acids usually includes the initial detection of the appropriate metal cations, and in the second stage, the obtained

in situ complex interacts with amino acid via displacement approach. A more complex problem is the creation of chemosensors capable of forming covalent bonds with the analyzed amino acid.

Amino acids are part of macromolecular proteins and represent essential substances for the growth and development of the human body. Cysteine (Cys) is of great importance in age defying, skin whitening, detoxifying, and improving immunity. Its deficiency causes premature senility, skin lesions, and uremia, while its excess can lead to senile dementia, neural tube defects, and osteoporosis. Histidine (His) is extremely important for the absorption of Fe^{2+} cations, vasodilation, and lowering blood pressure. The lack of His increases the risk of developing epilepsy, rheumatoid arthritis, and red cell aplasia, although its excessive content is associated with chronic kidney disease and Alzheimer's disease. Arginine (Arg) plays a vital role in cell replication, wound healing, and protein synthesis.

A simple coumarin sensor **29** selectively detects Hg^{2+} and Cys in an aqueous solution [58] (**Figure 28**). The addition of Hg(II) leads to a hypsochromic shift of the fluorescence emission band, while Cys almost completely quenches the emission of **29**. The latter process is seen by the naked eye under UV irradiation. The detection limit of **29** toward Cys is 8 μmol/L.

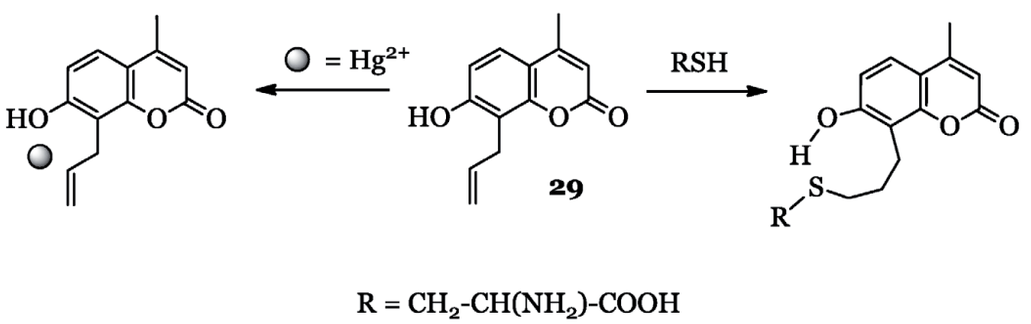

Figure 28.
Sensing mechanism of **29.**

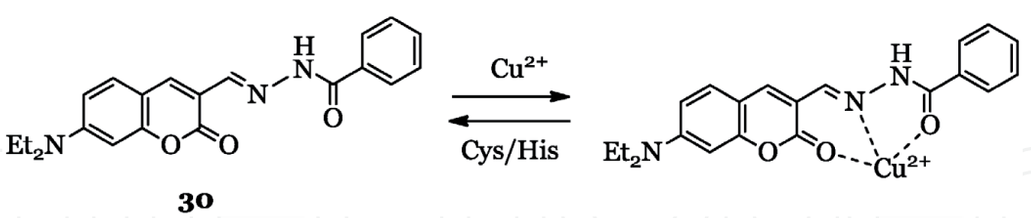

Figure 29.
Sensing mechanism of **30.**

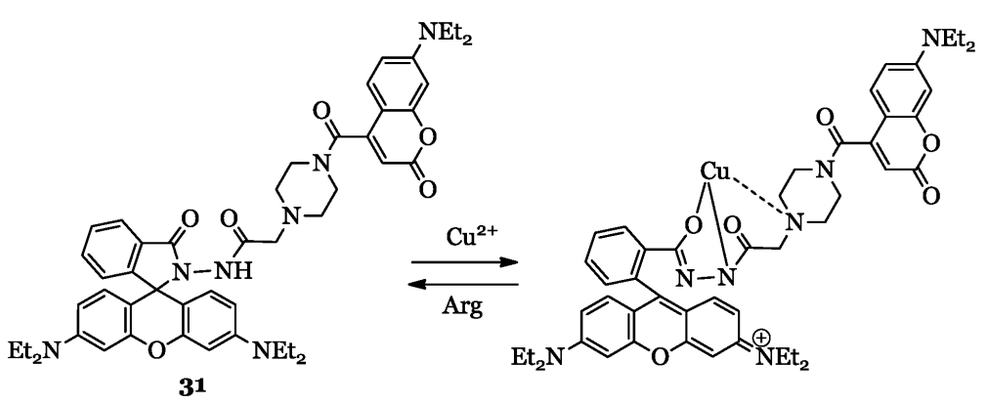

Figure 30.
Sequential detection of Cu^{2+} *and Arg by* **31.**

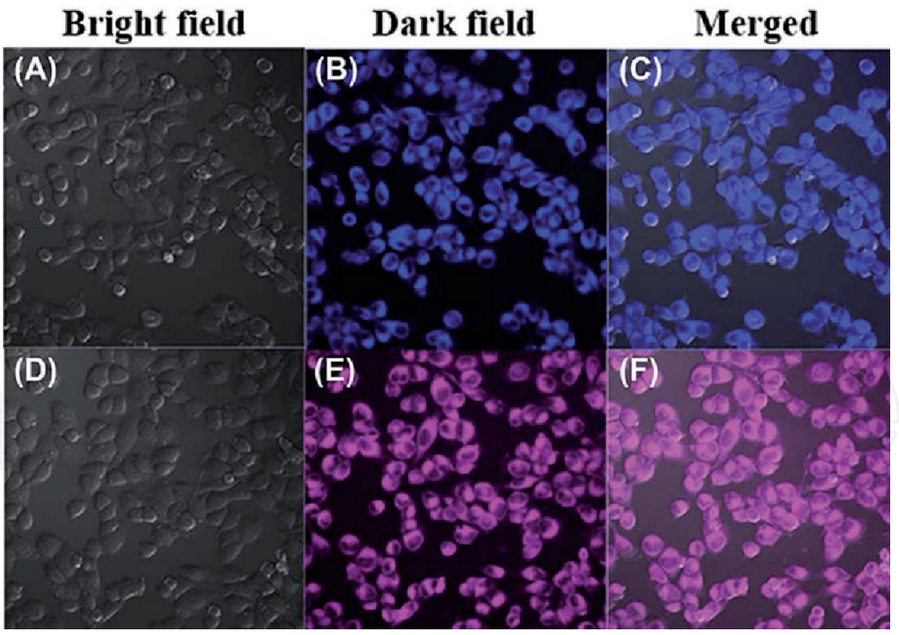

Figure 31.
Confocal fluorescence images of HeLa cells incubated with **31** *(20 mM) for 30 min (A–C) and then treated with* Cu^{2+} *(2 mM) for another 30 min (D–F). Images were obtained using an excitation of 405 nm and emission channels of (B) at 430–530 nm and (E) at 550–650 nm; (C and F) merge images of (A, B and D, E); (A and D) bright-field images of the cell culture [60].*

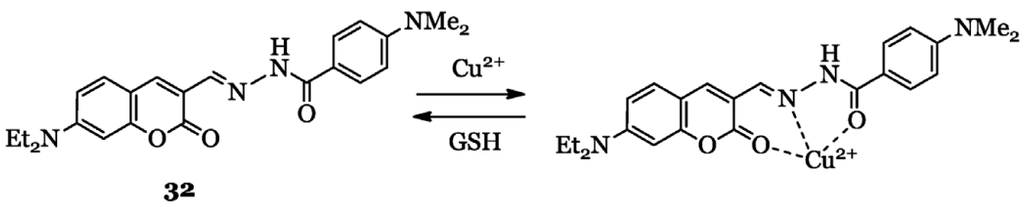

32

Figure 32.
Sequential detection of Cu^{2+} *and GSH by* **32.**

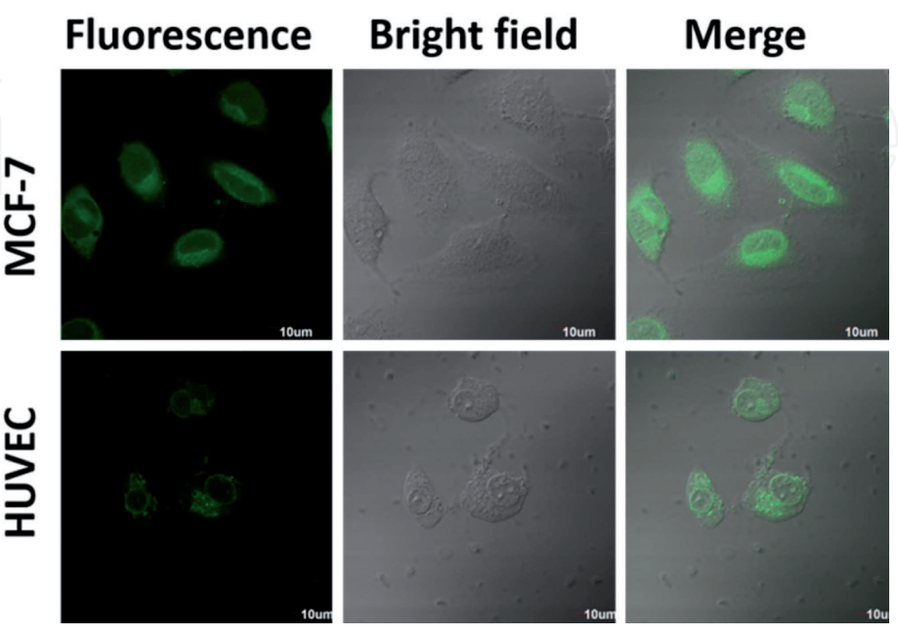

Figure 33.
Comparison of endogenous GSH level in MCF-7 and HUVEC cells after incubation with **32**-Cu^{2+} *complex. Left: Fluorescence images; middle: Bright-field images; right: Merged images [61].*

Coumarin **30** possesses a strong green emission at 527 nm [59]. Upon the addition of Cu^{2+}, **30** displays a significant fluorescence quenching. After the addition of Cys or His, the initial fluorescence is recovered due to the liberation of **30** (**Figure 29**).

Living A549 cells incubated with **30** exhibit notable emission. This fluorescence is quenched almost completely upon addition of Cu^{2+}. Further incubation of cells with Cys and His leads to the restoration of the initial fluorescence.

With the addition of Cu^{2+}, the solution of coumarin-rhodamine hybrid **31** in CH_3CN—H_2O mixture exhibits a naked-eye change from pale yellow to pink [60] (**Figure 30**). The fluorescence color converses from blue to pink (new maxima appear at 490 and 615 nm, which correspond to the emission of coumarin and rhodamine B moieties, respectively). The LOD for Cu^{2+} is 0.47 mM. The **31**-Cu^{2+} complex sequentially detects Arg with the restoration of blue fluorescence. The LOD for Arg is 0.33 mM.

The HeLa cells were incubated with **31** (20 mM) for 30 min, and a strong blue emission of the coumarin group was observed. Upon addition of Cu^{2+}, the HeLa cells exhibit strong pink fluorescence. These data show that **31** is cell permeable and can be applied to fluorescence imaging of intracellular Cu^{2+} (**Figure 31**).

Coumarin **32** was prepared for the detection of Cu^{2+} and glutathione (γ-glutamylcysteinylglycine, GSH) [61]. Overexpression of tumor biomarker GSH was found in many types of cancer. In the presence of Cu^{2}, **32** exhibits selective fluorescence quenching and color change from yellow to orange-red. When GSH was added to the solution, the initial fluorescence was recovered (**Figure 32**).

The LODs were calculated as 2.40×10^{-8} M and 1.29×10^{-7} M for Cu^{2+} and GSH, respectively.

MCF-7 and HUVEC cells were both incubated with **32**-Cu^{2+} complex for 30 min and then imaged under the same conditions (**Figure 33**). The fluorescence intensity in MCF-7 cells was above twofold higher than that in HUVEC cells, suggesting a higher GSH concentration in tumor cells. This is probably due to generation of additional GSH in tumor cells for resisting intrinsic oxidative stress.

Chemosensor **33** was designed for simultaneous detection of Cys, Hcy (homocysteine), and GSH [62]. Due to different binding mechanisms, compound **33** demonstrates enhancing of fluorescence intensity with 108-, 128-, and 30-fold at 457, 559, and 529 nm for Cys, Hcy, and GSH, respectively, through different excitation wavelengths (**Figure 34**).

For exogenous biothiols, the BEL-7402 cells were firstly pretreated with NEM and cellular biothiols and SH-containing proteins were deactivated. After incubation with **33**, no fluorescence could be observed (**Figure 35**).

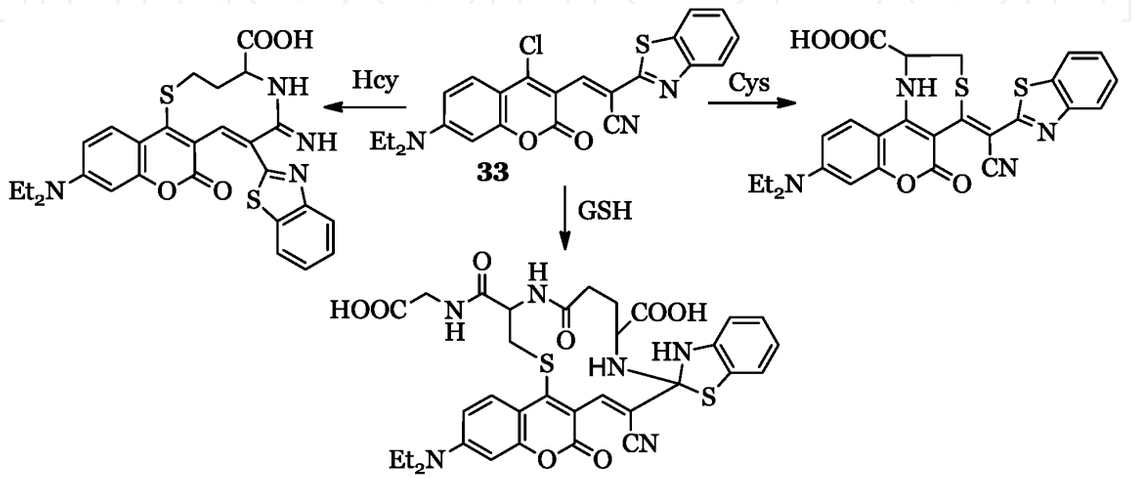

Figure 34.
Proposed mechanisms of bonding **33** *with Cys, Hcy, and GSH.*

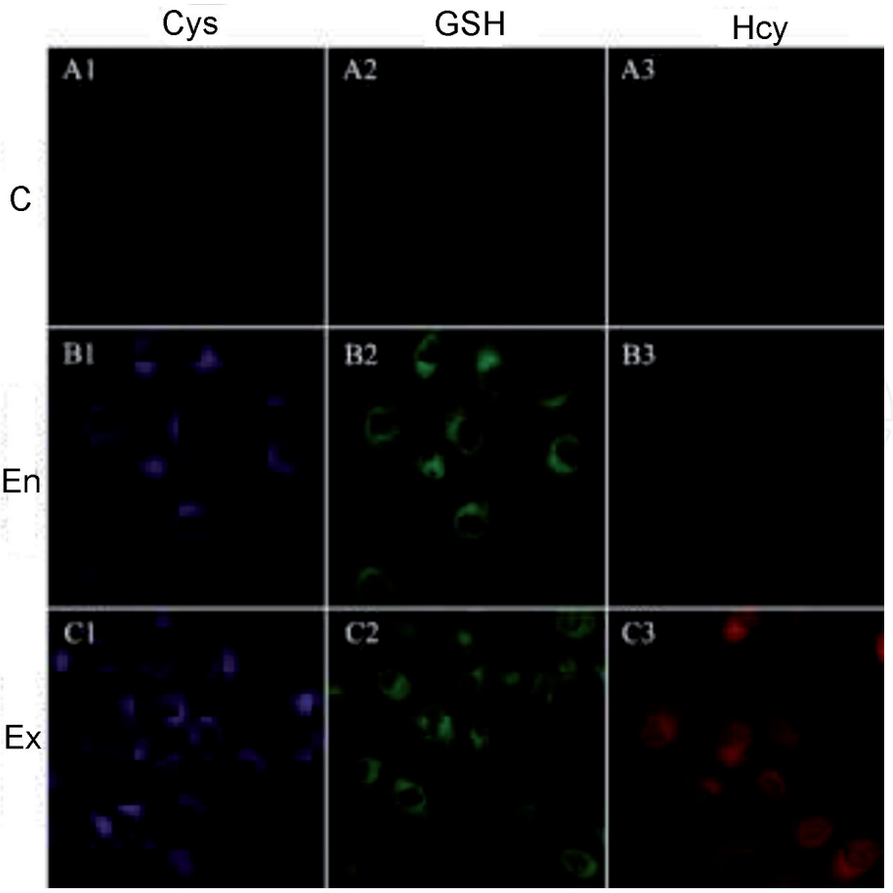

Figure 35.
Confocal fluorescence images of Cys, GSH, and Hcy in BEL-7402 cells. C: Control, en: Endogenous, ex: Exogenous. (A1–A3) cells were incubated for 30 min, then imaged. (B1–B3) cells were incubated with **33** *(2.5 μM) for 30 min, then imaged. (C1–C3) cells were pretreated with NEM (0.5 mM, 30 min), subsequently incubated with Cys/GSH/Hcy (500 μM, 30 min) and* **33** *(2.5 μM, 30 min), then imaged (λ_{ex} = 405 nm, λ_{em} = 421–475 nm for the blue channel; λ_{ex} = 458 nm, λ_{em} = 500–550 nm for the green channel; and λ_{ex} = 543 nm, λ_{em} = 552–617 nm for the red channel). Scale bar: 20 μm [62].*

After subsequent treatment with Cys, Hcy, and GSH, respectively, blue, red, and green fluorescence was observed from three different emission channels in living cells with high selectivity.

6. Conclusion

The design, synthesis, and investigation of fluorogenic polyfunctional coumarin chemosensors for multianalyte detection is an intriguing and extensively developing area of organic, medical, and biological chemistry. These sensors demonstrate high efficiency and selectivity combined with low cost and simplicity of analysis. Due to the limited size of the chapter, only sensors for the detection of metal cations, anions, and amino acids were considered, while sensors for proteins, DNA, RNA, etc. were ignored. Nevertheless, these data suggest that this group of polyfunctional chemosensors is extremely suitable for express analysis and bioimaging of various objects.

Acknowledgements

This research was financially supported by the Ministry of Science and Higher Education of the Russian Federation, project 0852-2020-2100-19. A. Dubonosov

worked in the framework of the State assignment of the Southern Scientific Centre of the RAS No. 01201354239.

Conflict of interest

The authors declare "no conflict of interest."

Author details

Alexander Dubonosov[1*] and Vladimir Bren[2]

1 Federal Research Centre the Southern Scientific Centre of the Russian Academy of Sciences, Rostov on Don, Russian Federation

2 Institute of Physical and Organic Chemistry, Southern Federal University, Rostov on Don, Russian Federation

*Address all correspondence to: aled@ipoc.sfedu.ru

References

[1] Anslyn EV, Wang B. Chemosensors: Principles, Strategies, and Applications. Hoboken: Wiley; 2011. p. 540 DOI: 10.1002/97811180195802

[2] Singh R, Das G. Towards fluorogenic and chromogenic sensing of heavy metal ions in aqueous medium: A mini-review. In: Singh DK, Das S, Materny A, editors. Advances in Spectroscopy: Molecules to Materials. Singapore: Springer Nature; 2019. pp. 57-65

[3] Suganya S, Naha S, Velmathi S. A critical review on colorimetric and fluorescent probes for the sensing of analytes via relay recognition. ChemistrySelect. 2018;**3**(25):7231-7268. DOI: 10.1002/slct.201801222

[4] Liu Z, He W, Guo Z. Metal coordination in photoluminescent sensing. Chemical Society Reviews. 2013;**42**(4):1568-1600. DOI: 10.1039/c2cs35363f

[5] Yu L, Wang S, Huang K, Liu Z, Gao F, Zeng W. Fluorescent probes for dual and multi analyte detection. Tetrahedron. 2015;**71**(29):4679-4706. DOI: 10.1016/j.tet.2015.04.115

[6] Wu J, Kwon B, Liu W, Anslyn EV, Wang P, Kim JS. Chromogenic/fluorogenic ensemble chemosensing systems. Chemical Reviews. 2015;**115**(15):7893-7943. DOI: 10.1021/cr500553d

[7] Chhatwal M, Kumar A, Singh V, Gupta RD, Awasthi SK. Addressing of multiple-metal ions on a single platform. Coordination Chemistry Reviews. 2015;**292**:30-55. DOI: 10.1016/j.ccr.2015.02.009

[8] Singh H, Bhargava G, Kumar S, Singh P. Quadruple-signaling (PET, ICT, ESIPT, C=N rotation) mechanism-based dual chemosensor for detection of Cu^{2+} and Zn^{2+} ions: TRANSFER, INH and complimentary OR/NOR logic circuits. Journal of Photochemistry and Photobiology A. 2018;**357**:175-184. DOI: 10.1016/j.jphotochem.2018.02.030

[9] Penta S, editor. Advances in Structure and Activity Relationship of Coumarin Derivatives. Amsterdam: Elsevier-Academic Press; 2015. p. 190

[10] Calcio Gaudino E, Tagliapietra S, Martina K, Palmisano G, Cravotto G. Recent advances and perspectives in the synthesis of bioactive coumarins. RSC Advances. 2016;**6**:46394-46405. DOI: 10.1039/C6RA07071J

[11] Bräse S. Privileged Scaffolds in Medicinal Chemistry. Design, Synthesis, Evaluation. Cambridge: RSC; 2015. p. 476 DOI: 10.1039/9781782622246

[12] Anamika UD, Ekta JN, Sharma S. Advances in synthesis and potentially bioactive of coumarin derivatives. Current Organic Chemistry. 2019;**22**(26):2509-2536. DOI: 10.2174/1385272822666181029102140

[13] Grover J, Jachak SM. Coumarins as privileged scaffold for anti-inflammatory drug development. RSC Advances. 2015;**5**(49):38892-38905. DOI: 10.1039/C5RA05643H

[14] Emami S, Dadashpour S. Current developments of coumarin-based anti-cancer agents in medicinal chemistry. European Journal of Medicinal Chemistry. 2015;**102**:611-630. DOI: 10.1016/j.ejmech.2015.08.033

[15] Medina FG, Marrero JG, Macias-Alonso M, González MC, Córdova-Guerrero I, Teissier García AG, et al. Coumarin heterocyclic derivatives: Chemical synthesis and biological activity. Natural Product Reports. 2015;**32**(10):1472-1507. DOI: 10.1039/c4np00162a

[16] An R, Hou Z, Li JT, Yu HN, Mou YH, Guo C. Design, synthesis and biological evaluation of novel 4-substituted coumarin derivatives as antitumor agents. Molecules. 2018;**23**(9):E2281. DOI: 10.3390/molecules23092281

[17] Matos MJ, Vazquez-Rodriguez S, Fonseca A, Uriarte E, Santana L, Borges F. Heterocyclic antioxidants in nature: Coumarins. Current Organic Chemistry. 2017;**21**(4):311-324. DOI: 10.2174/1385272820666161017170652

[18] Kathiravan MK, Salake AB, Chothe AS, Dudhe PB, Watode RP, Mukta MS, et al. The biology and chemistry of antifungal agents: A review. Bioorganic and Medicinal Chemistry. 2012;**20**(19):5678-5695. DOI: 10.1016/j.bmc.2012.04.045

[19] Hassan MZ, Osman H, Ali MA, Ahsan MJ. Therapeutic potential of coumarins as antiviral agents. European Journal of Medicinal Chemistry. 2016;**123**:236-255. DOI: 10.1016/j.ejmech.2016.07.056

[20] Yamaji M, Hakoda Y, Okamoto H, Tani F. Photochemical synthesis and photophysical properties of coumarins bearing extended polyaromatic rings studied by emission and transient absorption measurements. Photochemical and Photobiological Sciences. 2017;**12**(4):555-563. DOI: 10.1039/c6pp00399k

[21] Al-Masoudi NA, Al-Salihi NJ, Marich YA, Markus T. Synthesis, and fluorescence properties of coumarin and benzocoumarin derivatives conjugated pyrimidine scaffolds for biological imaging applications. Journal of Fluorescence. 2015;**25**(6):1847-1854. DOI: 10.1007/s10895-015-1677-z

[22] Nazir R, Stasyuk AJ, Gryko DT. Vertically π-expanded coumarins: The synthesis and optical properties. Journal of Organic Chemistry. 2016;**81**(22):11104-11114. DOI: 10.1021/acs.joc.6b02094

[23] Wang ZS, Cui Y, Hara K, Dan-oh Y, Kasada C, Shinpo A. A high-light-harvesting-efficiency coumarin dye for stable dye-sensitized solar cells. Advanced Materials. 2007;**19**(8):1138-1141. DOI: 10.1002/adma.200601020

[24] Cao D, Liu Z, Verwilst P, Koo S, Jangjili P, Kim JS, et al. Coumarin-based small-molecule fluorescent chemosensors. Chemical Reviews. 2019;**119**(18):10403-10519. DOI: 10.1021/acs.chemrev.9b00145

[25] Katerinopoulos HE. The coumarin moiety as chromophore of fluorescent ion indicators in biological systems. Current Pharmaceutical Design. 2004;**10**(30):3835-3852. DOI: 10.2174/1381612043382666

[26] Formica M, Fusi V, Giorgi L, Micheloni M. New fluorescent chemosensors for metal ions in solution. Coordination Chemistry Reviews. 2012;**256**:170-192. DOI: 10.1016/j.ccr.2011.09.010

[27] Song Y, Chen Z, Li H. Advances in coumarin-derived fluorescent chemosensors for metal ions. Current Organic Chemistry. 2012;**16**(22):2690-2707. DOI: 10.2174/138527212804004544

[28] Sareen D, Kaur P. Strategies in detection of metal ions using dyes. Coordination Chemistry Reviews. 2014;**265**:125-154. DOI: 10.1016/j.ccr.2014.01.015

[29] Qin J, Fan L, Wang B, Yang Z, Li T. The design of a simple fluorescent chemosensor for Al^{3+}/Zn^{2+} via two different approaches. Analytical Methods. 2015;**7**(2):716-722. DOI: 10.1039/C4AY02351J

[30] Fu J, Chang Y, Li B, Wang X, Xie X, Xu K. A dual fluorescence probe for

Zn^{2+} and Al^{3+} through differentially response and bioimaging in living cells. Spectrochimica Acta A. 2020;**225**. Article 117493. DOI: 10.1016/j.saa.2019.117493

[31] Zhang Q, Ma R, Li Z, Liu Z. A multi-responsive crown ether-based colorimetric/fluorescent chemosensor for highly selective detection of Al^{3+}, Cu^{2+} and Mg^{2+}. Spectrochimica Acta A. 2020;**228**. Article 117857. DOI: 10.1016/j.saa.2019.117857

[32] Roy N, Dutta A, Mondal P, Paul PC, Singh TS. A new coumarin based dual functional chemosensor for colorimetric detection of Fe^{3+} and fluorescence turn-on response of Zn^{2+}. Sensors and Actuators B. 2016;**236**:719-731. DOI: 10.1016/j.snb.2016.06.061

[33] Roy N, Nath S, Dutta A, Mondal P, Paul PC, Singh TS. A highly efficient and selective coumarin based fluorescent probe for colorimetric detection of Fe^{3+} and fluorescence dual sensing of Zn^{2+} and Cu^{2+}. RSC Advances. 2016;**6**(68):63837-63847. DOI: 10.1039/C6RA12217E

[34] Wang L, Li W, Zhi W, Huang Y, Han J, Wang Y, et al. A new coumarin schiff based fluorescent-colorimetric chemosensor for dual monitoring of Zn^{2+} and Fe^{3+} in different solutions: An application to bio-imaging. Sensors and Actuators B. 2018;**260**:243-254. DOI: 10.1016/j.snb.2017.12.200

[35] He X, Xie Q, Fan J, Xu C, Xu W, Li Y, et al. Dual-functional chemosensor with colorimetric/ratiometric response to Cu(II)/Zn(II) ions and its applications in bioimaging and molecular logic gates. Dyes and Pigments. 2020;**177**. Article 108255. DOI: 10.1016/j.dyepig.2020.108255

[36] Kumar A, Mondal S, Kayshap KS, Hira SK, Manna PP, Dehaend W, et al. Water switched aggregation/disaggregation strategies of a coumarin-naphthalene conjugated sensor and its selectivity towards Cu^{2+} and Ag^{+} ions along with cell imaging studies on human osteosarcoma cells (U-2 OS). New Journal of Chemistry. 2018;**42**(13):10983-10988. DOI: 10.1039/c8nj01631c

[37] Xu P, Liu X, Zhao X, Zhu W, Fang M, Wu Z, et al. A dual-function chemosensor based on coumarin for fluorescent turn-on recognition of Hg^{2+} and colorimetric detection of Cu^{2+} in aqueous media. Journal of the Chinese Chemical Society. 2020;**67**(2):298-305. DOI: 10.1002/jccs.201900188

[38] Liu M, Xu Z, Song Y, Li H, Xian C. A novel coumarin-based chemosensor for colorimetric detection of Ag(I) ion and fluorogenic sensing of Ce(III) ion. Journal of Luminescence. 2018;**198**:337-341. DOI: 10.1016/j.jlumin.2018.02.047

[39] Puthiyedath T, Bahulayan D. A click derived triazole-coumarin derivative as fluorescence on-off PET based sensor for Ca^{2+} and Fe^{3+} ions. Sensors and Actuators B. 2018;**272**:110-117. DOI: 10.1016/j.snb.2018.05.126

[40] Yanar U, Babür B, Pekyilmaz D, Yahaya I, Aydiner B, Dede Y, et al. A fluorescent coumarin-thiophene hybrid as a ratiometric chemosensor for anions: Synthesis, photophysics, anion sensing and orbital interactions. Journal of Molecular Structure. 2016;**1108**:269-277. DOI: 10.1016/j.molstruc.2015.11.081

[41] Razi SS, Ali R, Srivastava P, Shahid M, Misra A. An efficient multichannel probe to detect anions in different media and its real application in human blood plasma. RSC Advances. 2014;**4**(43):22308-22317. DOI: 10.1039/c4ra02388a

[42] Şahin Ö, Özdemir ÜÖ, Seferoğlu N, Genc ZK, Kaya K, Aydiner B, et al. New platinum(II) and palladium(II) complexes of coumarin-thiazole Schiff base with a fluorescent chemosensor

properties: Synthesis, spectroscopic characterization, X-ray structure determination, in vitro anticancer activity on various human carcinoma cell lines and computational studies. Journal of Photochemistry and Photobiology B. 2018;**178**:428-439. DOI: 10.1016/j.jphotobiol.2017.11.030

[43] Padhan SK, Podh MB, Sahu PK, Sahu SN. Optical discrimination of fluoride and cyanide ions by coumarinsalicylidene based chromofluorescent probes in organic and aqueous medium. Sensors and Actuators B. 2018;**255**(2):1376-1390. DOI: 10.1016/j.snb.2017.08.133

[44] Islam M, Hameed A, Ayub K, Naseer MM, Hussain J, Alharthy RD, et al. Receptor-spacer-fluorophore based coumarin-thiosemicarbazones as anion chemosensors with "turn on" response: Spectroscopic and computational (DFT) studies. ChemistrySelect. 2018;**3**(26):7633-7642. DOI: 10.1002/slct.201801035

[45] Shan Y, Sun Y, Suna N, Guan R, Cao D, Wang K, et al. One diethylamine coumarin derivative with nitro substituted chalcone structure as chemosensor for cyanide and copper ions. Inorganic Chemistry Communications. 2015;**59**:68-70. DOI: 10.1016/j.inoche.2015.06.031

[46] Wang K, Feng W, Wang Y, Cao D, Guan R, Yu X, et al. A coumarin derivative with benzothiazole Schiff's base structure as chemosensor for cyanide and copper ions. Inorganic Chemistry Communications. 2016;**71**:102-104. DOI: 10.1016/j.inoche.2016.07.013

[47] Mukherjee S, Talukder S. A coumarin-based luminescent chemosensor for recognition of Cu^{2+} and its in-situ complex for CN-sensing via Cu^{2+} displacement approach. Journal of Fluorescence. 2017;**27**:1567-1572. DOI: 10.1007/s10895-016-1974-1

[48] Qin J, Yang Z. Design of a novel coumarin-based multifunctional fluorescent probe for Zn^{2+}/Cu^{2+}/S^{2-} in aqueous solution. Materials Science and Engineering C. 2015;**57**:265-271. DOI: 10.1016/j.msec.2015.07.064

[49] Feng Y, Yang Y, Wang Y, Qiu F, Song X, Tang X, et al. Dual-functional colorimetric fluorescent probe for sequential Cu^{2+} and S^{2-} detection in bio-imaging. Sensors and Actuators B. 2019;**288**:27-37. DOI: 10.1016/j.snb.2019.02.062

[50] Liu Z, Liu L, Li J, Qin Y, Zhao C, Mi C, et al. A new coumarin-based fluorescent probe for selective recognition of Cu^{2+} and S^{2-} in aqueous solution and living cells. Tetrahedron. 2019;**75**:3951-3957. DOI: 10.1016/j.tet.2019.05.057

[51] Gu L, Zheng T, Xu Z, Song Y, Li H, Xia S, et al. A novel bifunctional fluorescent and colorimetric probe for detection of mercury and fluoride ions. Spectrochimica Acta A. 2019;**207**:88-95. DOI: 10.1016/j.saa.2018.08.060

[52] Dubonosov AD, Bren VA, Minkin VI. Enolimine-ketoenamine tautomerism for chemosensing. In: Antonov L, editor. Tautomerism: Concepts and Applications in Science and Technology. Weinheim: Wiley-VCH; 2016. pp. 229-252. DOI: 10.1002/9783527695713.ch10

[53] Nikolaeva OG, Shepelenko EN, Tikhomirova KS, Revinskii YV, Dubonosov AD, Bren VA, et al. Bifunctional fluorescent and colorimetric "naked eye" aroylhydrazone chemosensors for Hg^{2+} and F^- ions detection. Mendeleev Communications. 2016;**26**(5):402-404. DOI: 10.1016/j.mencom.2016.09.012

[54] Nikolaeva OG, Karlutova OY, Dubonosov AD, Bren VA, Minkin VI. Synthesis and luminescence and ionochromic properties of

9-hydroxy-1-methyl-3-oxo-3H-benzo[f] chromene-8-carbaldehyde imines and hydrazones. Russian Journal of General Chemistry. 2020;**90**(2):196-201. DOI: 10.1134/S107036322002005X

[55] Meng X, Cao D, Hu Z, Han X, Li Z, Liang D, et al. A coumarin based highly selective fluorescent chemosensor for sequential recognition of Cu^{2+} and PPi. Tetrahedron Letters. 2018;**59**(49):4299-4304. DOI: 10.1016/j.tetlet.2018.10.048

[56] Zhao C, Chen J, Cao D, Wang J, Ma W. Novel coumarin-based containing denrons selective fluorescent chemosesor for sequential recognition of Cu^{2+} and PPi. Tetrahedron. 2019;**75**(13):1997-2003. DOI: 10.1016/j.tet.2019.02.024

[57] Li S, Cao D, Meng X, Hu Z, Li Z, Yuan C, et al. A novel fluorescent chemosensor based on coumarin and quinolinylbenzothiazole for sequential recognition of Cu^{2+} and PPi and its applicability in live cell imaging. Spectrochimica Acta A. 2020;**230**. Article 118022. DOI: 10.1016/j.saa.2019.118022

[58] Tao P, Chen D, Xu Z, Song Y, Li H, Xian C. A fluorescent probe for the dual detection of mercury ions and thiols based on a simple coumarin derivative. Coloration Technology. 2020;**136**(1):75-86. DOI: 10.1111/cote.12447

[59] Xie Y, Yan L, Li J. An on-off-on fluorescence probe based on Coumarin for Cu^{2+}, cysteine, and histidine detections. Applied Spectroscopy. 2019;**73**(7):794-800. DOI: 10.1177/0003702818821329

[60] Wang S, Ding H, Wang Y, Fan C, Liu G, Pu S. A colorimetric and ratiometric fluorescent sensor for sequentially detecting Cu^{2+} and arginine based on a coumarin-rhodamine B derivative and its application for bioimaging. RSC Advances. 2019;**9**(12):6643-6649. DOI: 10.1039/c8ra09943j

[61] Wang Z, Ding X, Huang Y, Yan X, Ding B, Li Q, et al. The development of coumarin Schiff base system applied as highly selective fluorescent/colorimetric probes for Cu^{2+} and tumor biomarker glutathione detection. Dyes and Pigments. 2020;**175**. Article 108156. DOI: 10.1016/j.dyepig.2019.108156

[62] Yin G, Niu T, Gan Y, Yu T, Yin P, Chen H, et al. A multi-signal fluorescent probe with multiple binding sites for simultaneous sensing of Cys, Hcy and GSH. Angewandte Chemie. 2018;**57**(18):4991-4994. DOI: 10.1002/anie.201800485